

## Strength grading of hardwoods using transversal ultrasound

Kovryga, Andriy; Khaloian Sarnaghi, A.; van de Kuilen, Jan-Willem

**Publication date**

2019

**Document Version**

Final published version

**Published in**

ISCHP 2019 - 7th International Scientific Conference on Hardwood Processing

**Citation (APA)**

Kovryga, A., Khaloian Sarnaghi, A., & van de Kuilen, J-W. (2019). Strength grading of hardwoods using transversal ultrasound. In J-W. van de Kuilen, & W. Gard (Eds.), *ISCHP 2019 - 7th International Scientific Conference on Hardwood Processing* (pp. 220-229). Delft University of Technology.

**Important note**

To cite this publication, please use the final published version (if applicable). Please check the document version above.

**Copyright**

Other than for strictly personal use, it is not permitted to download, forward or distribute the text or part of it, without the consent of the author(s) and/or copyright holder(s), unless the work is under an open content license such as Creative Commons.

**Takedown policy**

Please contact us and provide details if you believe this document breaches copyrights. We will remove access to the work immediately and investigate your claim.

## Strength grading of hardwoods using transversal ultrasound

A. Kovryga<sup>1\*</sup>, A. Khaloian Sarnaghi<sup>1</sup>, J-W. G. van de Kuilen<sup>1,2</sup>

<sup>1</sup> Wood Research Munich  
Technical University of Munich  
80797 Munich, Germany

<sup>2</sup> Faculty of Civil Engineering and Geosciences  
Technical University of Delft  
Delft, Netherlands

### ABSTRACT

*Detection of local wood inhomogeneities is important for accurate strength and stiffness prediction. In hardwood specimens, visual characteristics (e.g. knots or fibre deviation) are difficult to detect, either with a visual surface inspection or by the machine. Transversal ultrasound scan (TUS) is a non-destructive evaluation method with high potential for hardwoods. The method relies on differences in ultrasound wave propagation in perpendicular to the grain direction. The aim of this study is to estimate and analyse the capabilities of TUS for defect detection in hardwoods and prediction of mechanical property values. In the current paper, the TUS was applied to the hardwood species European ash (*Fraxinus excelsior*) and European maple (*Acer sp.*). In total, 16 boards of both specimens were completely scanned perpendicular to the grain using a laboratory scanner with dry-coupled transducers. The measurements were processed to 2D scan images of the boards, and image processing routines were applied to further feature extraction, defect detection and grading criteria calculation. In addition, as a reference for each board, all relevant visual characteristics and mechanical properties from the tensile test were measured. Using the TUS global fibre orientation, the size and the position of the knots can be detected. Knottiness correlates to the strength properties similarly or even better compared to the manual knottiness measurement. Between the global fibre orientation (measured using TUS and measured on the failure pattern) no correlation could be found. The ultrasound MOE perpendicular to the grain does not show any meaningful correlation to the elastic-properties parallel to the grain. In overall, TUS shows high potential for the strength grading of hardwoods.*

### 1. INTRODUCTION

Temperate European hardwoods, such as ash, beech and oak are known for excellent mechanical properties, which also make them attractive for structural applications. In order to utilize the advanced mechanical properties, the high variation of this naturally grown material needs to be reduced. For the strength of wood and, especially of hardwoods, visible local wood inhomogeneities are important. The same characteristics are more difficult to detect and measure with the available techniques compared to softwood (Olsson et al. 2018; Schlotzhauer et al. 2018).

The relationship between the grading criteria and the mechanical properties, as well as application of grading methods, differ between softwoods and hardwoods. The most accurate strength prediction method, at least for softwoods, is achieved by the means of the machine strength grading. The grading machines can explain up to 62% of the strength variation (Bacher 2008). For hardwoods machine grading allows only limited prediction accuracy. Models based on dynamic MOE ( $MOE_{dyn}$ ), most common criterion for the strength prediction, show  $R^2$  values between 0.18 and 0.36 (Nocetti et al. 2016; Ravenshorst 2015). Higher prediction accuracy can be achieved only if dynamic MOE is combined with visually measured knottiness (Frühwald and Schickhofer 2005; Kovryga et al. 2019). Machine detection of the knottiness works currently less accurate for hardwoods compared to softwoods. Grading machines that use x-ray for the knot detection are limited due to the low contrast between the knots and clear wood (Giudiceandrea 2005). Other methods are currently not available for the strength grading purposes.

Fibre deviation is another important criterion for the grading of hardwoods if strength is regarded. For defect free specimens with high variation in strength values fibre angle has major impact on the strength. Visible fibre angle provides no reliable results for the strength prediction (Frühwald and Schickhofer 2005). The machine detection of the fibre deviation by means of different non-destructive techniques has been recently in the scope of the study. For softwoods the multi-sensory systems able to detect the fibre deviation by the means of tracheid effect are available

---

\* Andriy Kovryga: Tel.: +49 89 2180 6473; E-mail: kovryga@hfm.tum.de

(Olsson et al. 2013). Application of other NDT techniques on hardwoods, such as thermal conductivity measurement (Daval et al. 2015). 2015) and automated visual analysis of the spindle patterns (Ehrhart et al. 2018) has been on the research agenda.

A possible technology for cost-efficient and precise strength grading of timber is transversal ultrasound scan (TUS). The common way to use ultrasound for strength grading is to determine velocity of the ultrasound wave in longitudinal to the grain direction and therefore  $MOE_{dyn}$  (Sandoz 1989). By applying ultrasound perpendicular to the grain direction defects in wood can be detected. TUS has been reported to detect the knots in softwoods and some Northern American hardwoods in pallet parts (Kabir et al. 2002; Kabir et al. 2003) and structural timber (Machado et al. 2004). Ultrasound provides also information on the growth ring alignment. Propagation of the ultrasound wave differs between the radial and tangential growth ring orientation e.g. (Bucur 2006). Yaitskova and van de Kuilen (2014) provides analytical model that links ultrasound wave propagation and growth ring orientation, so called radial-tangential profile (RT-profile) and also highlights the possible application of TUS for the strength grading.

The aim of the present study is to analyze the potential of TUS for the grading of European hardwoods ash and maple. Particularly, is the definition and application of the novel grading criteria of interest. The possibility to detect the major grading criteria - knots and the fibre deviation – and relate them to the mechanical properties are within the scope of the study.

## 2. MATERIALS

To study the potential of ultrasound scan in overall 16 lamellas of European softwoods and hardwoods were used. Table 1 gives an overview of the selected specimens of the species European ash (*Fraxinus excelsior*), maple (*Acer spp.*). The selected specimens are part of a larger sampling presented in Kovryga et al. (2019) for hardwoods. The material can be considered representative for the selected species grown in central Europe. The boards were selected in a way that different wood features such as presence of the pith, knots, fibre deviations, as well as defect free specimens were present in a sample. The growth ring orientation affects the propagation time of the ultrasound wave.

Table 1: Number, dimensions and mechanical properties of scanned European ash (*Fraxinus excelsior*) and maple (*Acer spp.*) boards

| Wood species | Number (n) | Cross-sections $b \times h$ [mm x mm] | Scan length [mm] | tKAR [-] |       | $\rho$ [kg/m <sup>3</sup> ] |    | $E_0$ [GPa] |     | $f_t$ [MPa] |      |
|--------------|------------|---------------------------------------|------------------|----------|-------|-----------------------------|----|-------------|-----|-------------|------|
|              |            |                                       |                  | $\mu$    | s     | $\mu$                       | s  | $\mu$       | s   | $\mu$       | s    |
| Ash          | 3          | 30 x 125                              | 1125             | 0.090    | 0.081 | 692                         | 43 | 16.9        | 1.5 | 71.0        | 17.8 |
|              | 4          | 35 x 125                              | 1125             |          |       |                             |    |             |     |             |      |
| Maple        | 2          | 25 x 125                              | 1125             | 0.208    | 0.117 | 664                         | 23 | 14.1        | 1.8 | 39.1        | 15.8 |
|              | 3          | 30 x 125                              | 1125             |          |       |                             |    |             |     |             |      |
|              | 4          | 35 x 125                              | 1125             |          |       |                             |    |             |     |             |      |
|              | 63*        | 35 x 100                              | 900              |          |       |                             |    |             |     |             |      |
| Total        | 80         |                                       |                  |          |       |                             |    |             |     |             |      |

## 3. METHODS

### 3.1. TRANSVERSAL ULTRASOUND SCAN (TUS)

The hardwood specimens were scanned using laboratory scanner developed at the TU Munich (Figure 1). The measuring unit (ultrasound transducers) are moved along the specimen in x and y-direction within the scan area. Measuring unit used to measure and generate ultrasound signal included Pundit Lab+ with two dry-contact piezoceramic transducers, with a central frequency of 54 kHz from PRECEQ.

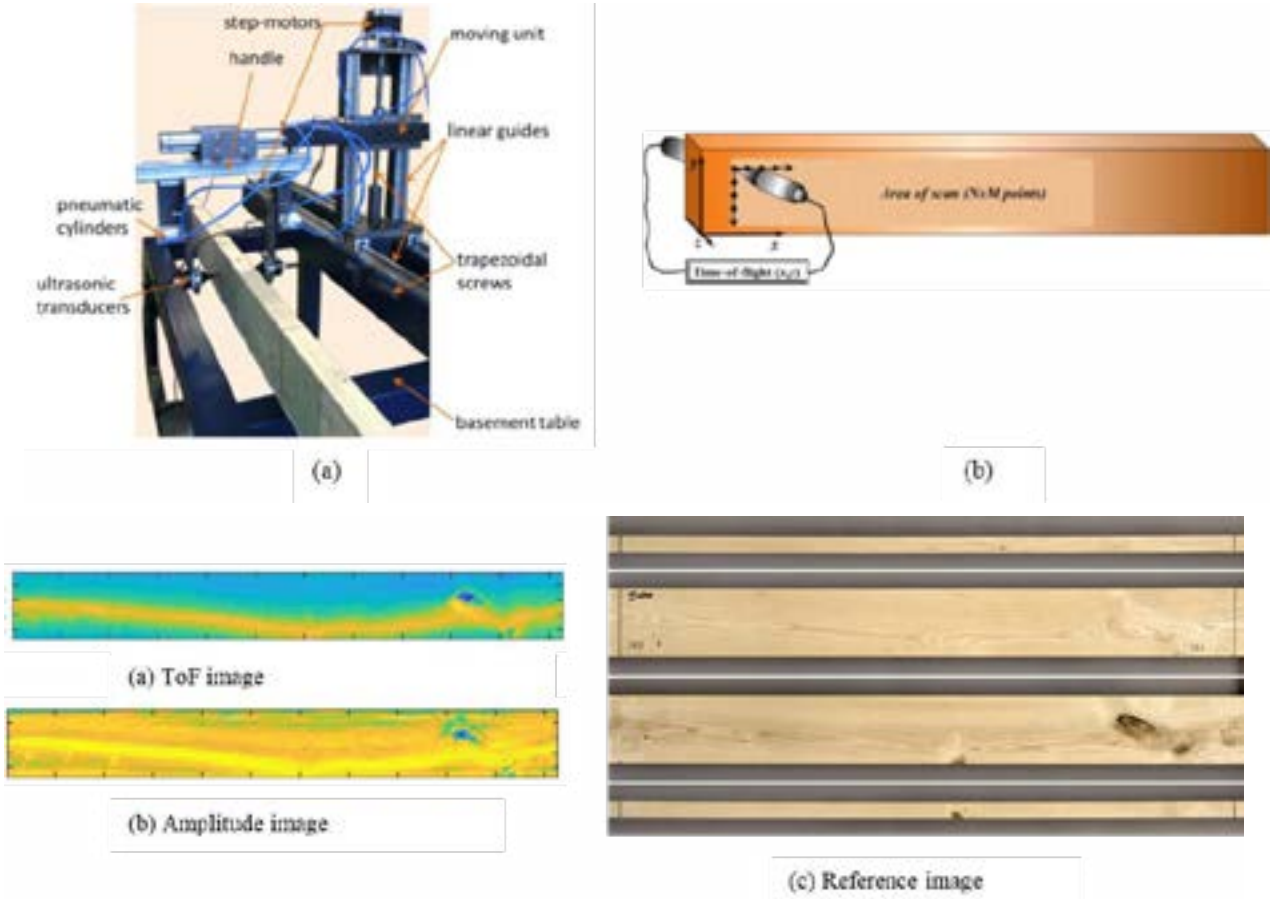
For each specimen, the area of 9 times the width was scanned by the device resulting in total of 82800 measuring points. For each measuring points different parameters of us signal – ToF, amplitude, energy, and spectral density – were calculated. For each parameter, a 2D image was generated and used to distinguish between the wood features and clear wood using image processing algorithms and optimization routines (Figure 2). For the current analysis only ToF is used. The ToF was calculated using threshold value of the signal amplitude. When the signal exceeds the threshold, the time is measured as ToF. Based on cluster-analysis we came to the conclusion that for 54 kHz transducer

\*scanned with a coarse grid to evaluate relationship between  $E_{us,90}$  to  $E_0$

only time-of-flight provides sufficient results for the defect detection. Other parameters (such as amplitude in Figure 2b) did not provide any additional information on the defects.

Figure 1: Mechanical structure of TUS (a) and the measuring geometry (b) (Yaitskova et al. 2015)

Figure 2: Scan images for the European ash (*Fraxinus excelsior*) specimen Nr. 263 (a) time-of-flight (ToF) and (b) amplitude in



comparison to the images of the scan area acquired on all four surfaces (c)

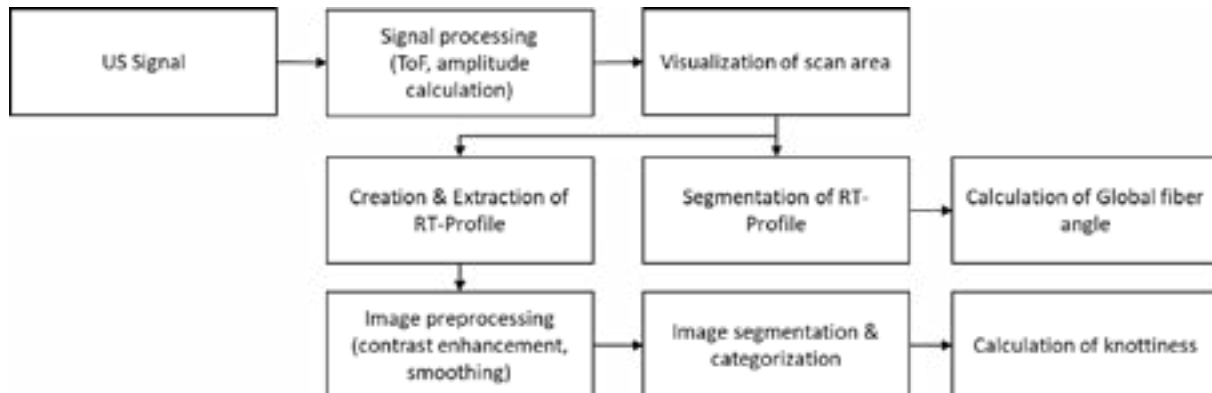


Figure 3: Algorithm for the processing of the ultrasound images

### 3.2. PROCESSING OF ULTRASOUND IMAGES

#### 3.2.1 IMAGE PROCESSING

In current study the feature detection includes two major targets: the detection of the global fibre deviation (minimum of RT-profile) and the detection of defects such as knots. Figure 3 visualizes major steps in processing of ultrasound signal starting with the measurement of ultrasound signal, over signal processing to the visualization and image processing steps required to segment the selected wood features (knots and alignment of fibres) out of the image. Each board is processed separately. For the implementation the MATLAB Image Processing Toolbox ver. 2016a with image were used. The major steps are highlighted in following:

**1. RT-profile extraction.** In original time of flight (ToF) image beside the wood features the macroscopic growth ring orientation can be observed. The speed of ultrasound wave differs dependent on the propagation direction and is greater in radial than in tangential direction. These differences between radial and tangential orientation, named RT-profile, is shown in Figure 2a as gradient. This alignment coincides with the position of the knots and needs to be filtered. Yaitskova and van de Kuilen (2014) suggested analytical approach to extract the profile. However, this approach requires fitting the polynomial to each tested specimen. In the current study the RT-profile was restored by applying the median filter with the 3x10 mask to the ToF image and extracting it (Eq. 1). Applying filter over the length allowed to exclude local wood features, such as knots. Similar approach was chosen by Machado et al. (2004) to normalize the wave parameters and reduce the influence of structural features from timber pieces.

$$D(x, y) = M_{tof}(x, y) - F(x, y) \quad (1)$$

where D is a filtered image,  $M_{tof}$  is original image and F is medium filter applied to it.

**2. Image preprocessing.** Extraction of the profile increased the noise level in the image. To improve the segmentation performance blurring using “wiener filter” was applied to the images after RT-profile extraction. Wiener filter provides good solution for noisy images by adaptively tailoring itself to the local image variance. Where the variance is large only little smoothing is done; where the variance is little more smoothing is performed. The mask of 3x10 pixels was chosen for the filtering. This means that the filter was applied in 10 pixels over the length of the board and 3 pixels in the height.

**3. Segmentation.** Segmentation is the process of objects extraction out of the image. Various algorithms, such as threshold techniques, texture-based algorithms, wavelet-based techniques, are available. Algorithms are suitable to some specific use cases. Threshold technique are the most common and frequently used techniques for low noise levels. For the current study, the segmentation was done using global threshold value. Binary map is created by the global thresholding technique. By exceeding certain threshold value pixels are either assigned to defects or clear wood. Map is created as follows:

$$B_{tof}(x, y) = \begin{cases} 1 & \text{if } D(x, y) \geq T, \text{ defect} \\ 0 & \text{if } D(x, y) < T, \text{ clear wood} \end{cases} \quad (2)$$

Threshold (T) is a threshold value calculated for each single board as follows:

$$T = \mu \pm s \quad (3)$$

Where  $\mu$  is the mean value and s standard deviation of values in filtered image D.

**4. Classification.** Classification is an important step to assign the object to the specific defect type based on the features of the segmented region. The boards included mostly knots and drying cracks in knots. No cracks were observed within the boards. Due to the low number of defect classes (clear wood vs knots) and only limited number of boards no specific classification routine has been applied. Applying classification routines such as kNN-classifier (k- nearest neighbor) or Neuronal networks might improve the classification result, would, however, require larger data set.

### 3.2.2 DETECTION OF RT-PROFILE

Each measurement of the ultrasound wave between the sender and receiver integrates both macroscopic profile and the effect of wood features. Such overlapping may lead to unreliable defect detection and classification, as well difficulties in profile detection.

Different solutions were tested for the RT-profile detection. One possibility to detect the RT-profile is to calculate the minima of the ToF at each single crosscut over the length of the test sample. In this case, for some crosscuts instead of the minimum of the RT-profile, the wood inhomogeneities were detected. Also image processing techniques, and particularly edge detection algorithm, were tested for the fibre alignment detection. Edge detection uses discontinuities in brightness to detect the boundaries of the object. Such contrast is observable at the minima of the RT-profile.

However, presence of the knots and in some cases low contrast did not allow for the continuous and consistent fibre alignment identification.

The best solution was to detect the RT-Profile by calculating the weighted minimum of ToF at a given point over the length of the board. The weight assured that abrupt changes in RT-profile do not occur. The minimum of RT-Profile in position  $x$  is calculated using following equation:

$$P_x = \min(W(x, y) \cdot M_{tof,x}) \quad (4)$$

The weights  $W$  at the length coordinate  $x$  are calculated using Eq. 5.

$$W(x, y) = \left( 1 + \frac{|P_{(x,y)} - P_{x-1}|}{z} \right) \quad (5)$$

where  $P_{x-1}$  position of the minimum of the RT-profile in previous  $x$  position and  $z$  – distance between the RT-profile and board edge.

The calculation procedure is performed stepwise from the beginning of the board to the end. The selected approach ensures continuous path of RT-Profile within the board.

The grain angle is calculated as follows:

$$\alpha_{us} = \tan\left(\frac{\Delta y}{\delta}\right) \quad (6)$$

Where  $\delta$  is window size used for the calculation of the fibre angle and  $\Delta y$  is the distance in  $y$  plane (width of the specimen between the beginning ( $P_x$ ) and the end of the window ( $P_x + \delta$ )). Window size was set to 150mm.

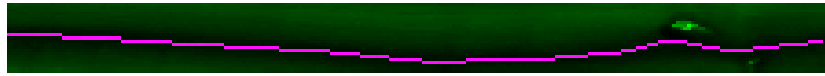


Figure 4: Minimum of the RT profile representing the fibre for the ash specimen 263

### 3.2.3 KNOTTINESS

Ultrasound knottiness was calculated based on the processed ToF images ( $B_{tof}$ ) and is defined as an area of the knot related to the reference area. Knottiness value at the location  $x$  is calculated using Eq. 7.

$$KAR_{us}(x) = \frac{\int_0^w B_{tof}(x, y) dy}{w} \quad (7)$$

Where  $w$  is the width of the board.

The knottiness of the board is calculated as maximum of running average in a 150 mm window ( $\delta$ ) over the length of the board or within a tension range as a maximum of a running average.

$$KAR_{us} = \max \frac{1}{\delta} \int_{x=\bar{x}-\delta/2}^{x=\bar{x}+\delta/2} KAR_{us}(x) dx \quad (8)$$

### 3.2.4 MOE PERPENDICULAR TO THE GRAIN

Additionally, the Modulus of elasticity perpendicular to the grain has been calculated. With knowledge of density and ultrasound velocity the MOE perpendicular to grain ( $E_{us,90}$ ) has been calculated:

$$E_{us,90} = v_{us} \cdot \rho \quad (9)$$

For the large maple sample ( $N = 63$ ) the ultrasound velocity ( $v_{us}$ ) was measured in 150 mm distance over the length of the board in four rows, with space 22.5 mm in between. In total 28 measurement points were measured for each board.

### 3.4 REFERENCE MEASUREMENTS

As the reference to the TUS, the visual quality of boards was assessed by measuring size and location of knots ( $d > 5$  mm), cracks and fibre deviation. To quantify the knottiness, the  $tKAR$  (*total Knottiness Area Ratio*) parameter was used.  $tKAR$  is calculated as area of knots appearing in 150mm large window, projected on the cross sectional area. The overlapping areas are counted once. Additionally, the fibre deviation was determined after the destructive test on the failure pattern. Fibre deviation is defined as an angle with the longitudinal axis of the sawn piece and is measured in % (grain angle). Furthermore, each scanned board was tested destructively in tension parallel to the grain in acc. with EN 408 (2010), with tensile strength and stiffness determined after conditioning under the reference conditions 20 °C and 65 % rel. humidity.

#### 4. RESULTS & DISCUSSION

Ultrasound transversal to the grain scan allows the detection of characteristics relevant for the strength of hardwoods. As already mentioned knots and global fibre orientation can be detected and extracted from the ultrasound scan images. The results and some pre-processing steps can be observed in Figure 4 for ash specimen. The knots can be visualized in ultrasound scan images. Furthermore, the global fibre-deviation can be observed and detected. The visibility of the fibre orientation is referred to the differences in the ultrasound wave propagation in radial and tangential direction. The knot detection works not smooth in every case.

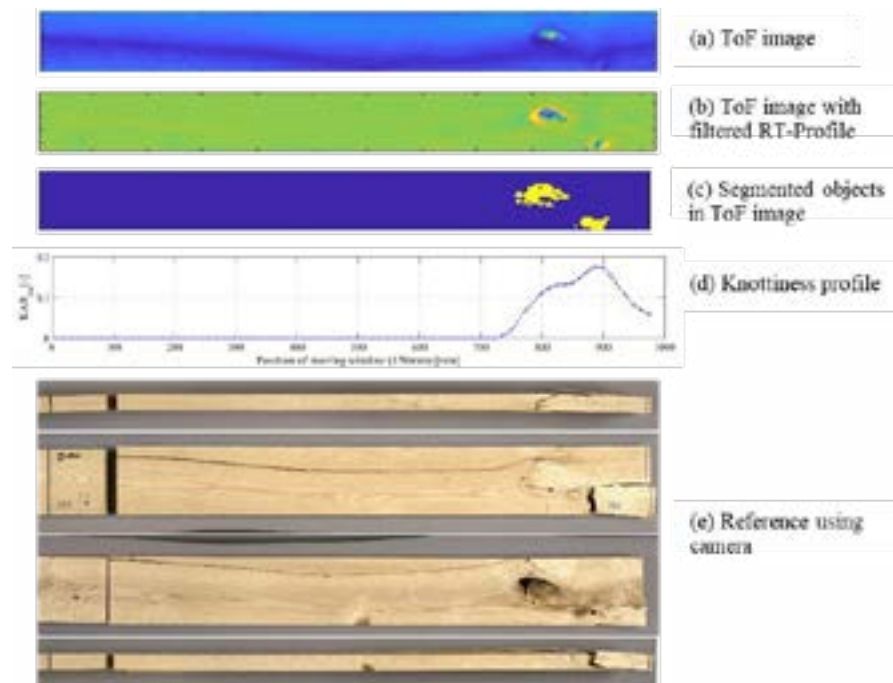


Figure 5: Ultrasound scan of ash specimen nr. 263 with (a) Original ToF image; (b) ToF image with extracted RT-Profile; (c) segmented objects in image; (d) Knottiness profile; (e) Reference image

Table 2: Correlations between ultrasound parameters, visual properties and mechanical properties for combined sample of European ash (*Fraxinus Excelsior*) and maple (*Acer spp.*) ( $N = 16$ )

|                  | $KAR_{us}$ | $\alpha_{us}$ | $tKAR$  | $\alpha_{break}$ | $\rho$ | $E$    | $f_i$    |
|------------------|------------|---------------|---------|------------------|--------|--------|----------|
| $KAR_{us}$       | 1          | 0.353         | 0.791** | 0.235            | -0.177 | -0.401 | -0.781** |
| $\alpha_{us}$    |            | 1             | 0.459   | 0.814**          | -0.171 | -0.462 | -0.388   |
| $tKAR$           |            |               | 1       | 0.516*           | 0.019  | -0.469 | -0.737** |
| $\alpha_{break}$ |            |               |         | 1                | -0.170 | -0.484 | -0.341   |
| $\rho$           |            |               |         |                  | 1      | 0.508* | 0.178    |
| $E$              |            |               |         |                  |        | 1      | 0.619**  |
| $f_i$            |            |               |         |                  |        |        | 1        |

Note: \* $p < 0.05$ , \*\* $p < 0.01$

#### 4.1. KNOTTINESS

The knottiness from ultrasound image shows high correlation to the visually measured knottiness ( $r = 0.791$ ). The scatter shows positive relationship between  $KAR$  values from TUS measurement and  $tKAR$  and the clear trend line can be registered (Figure 6). It also appears that for one specimen the knottiness has been detected, although no knots were visually observable within the specimen. By studying the test specimen carefully, we detected pith on the surface of the board with groove that has led to an increase in time of flight value due to the missing contact between the surface and transducer. Applying classification routine would allow to avoid such misclassification and/or classify such features separately. Selected approach would allow applying the classification on the detected object and not to the single measurement. This spatial information would allow to increase the accuracy.

The relationship between the knottiness parameters and tensile strength can be observed in Figure 7. For both TUS knottiness and manually measured knottiness  $tKAR$  the tensile strength decreases with an increase in knottiness values. The prediction accuracy is in both cases high ( $R^2 > 0.5$ ). TUS knottiness shows significantly higher  $R^2$  values compared to the  $tKAR$ . The residuals scatter less around the regression line in case of the TUS knottiness compared to the visually determined knottiness. The results should be taken indicative only, as only limited number of specimens are scanned.

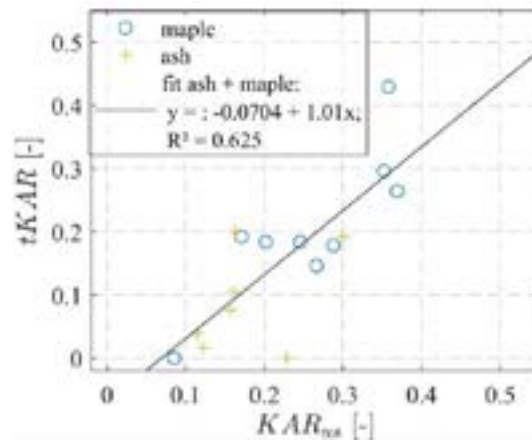


Figure 6: Scatter plot between knottiness parameter  $KAR_{us}$  estimated from the ultrasound scan and the manually measured knottiness  $tKAR$

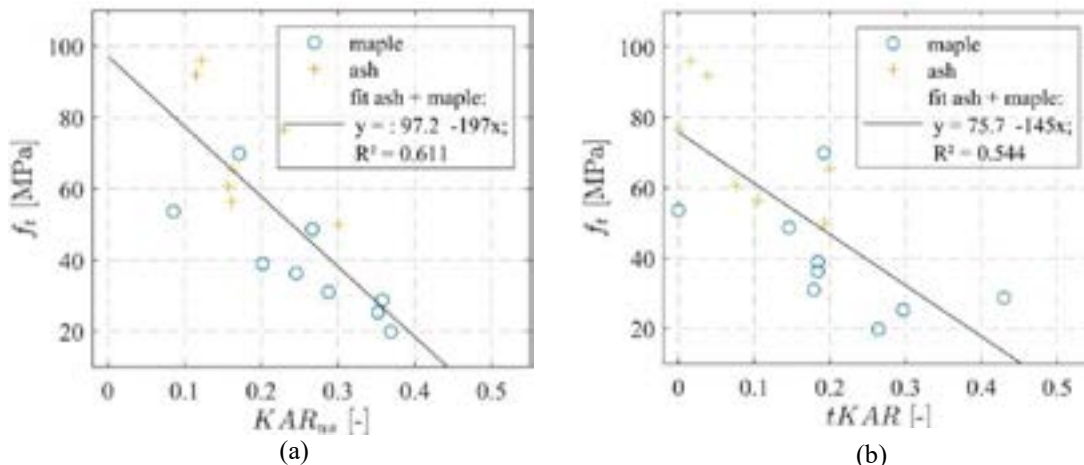


Figure 7: Relationship between (a) knottiness measured using ultrasound device and tensile strength and (b) manually measured knottiness ( $tKAR$ ) and tensile strength for European ash and maple



4.2 GLOBAL FIBRE DEVIATION DETECTION

Fibre deviation is an important grading parameter for hardwoods. As shown previously the ultrasound is able to detect the minimum of the so-called RT-Profile that indicates the alignment of fibres in board. The ultrasound wave propagates in radial direction faster than in tangential direction. Figure 8 shows the relationship between fibre deviation measured using ultrasound and the fibre deviation detected manually by observing the failure pattern. The relationship is linear, between the two measurement methods. For most of the specimens, the fibre angle ranged between 3 to 10 %. For two boards greater fibre deviation was indicated using both methods. The small sample allows only indicative conclusions. The difference between the two measurements arises from the nature of the measurement. In case of ultrasound, the fibre angle measurement is an integral over the depth of the board.

Relationship between fibre angle and tensile strength is similar for both measurements. Clear decrease in tensile strength for decreasing fibre angle can be observed (Figure 9). However, there no significant correlation between the fibre angle (measured using TUS device and measured manually on the failure pattern) and strength. For fibre deviations of 10% and lower the residuals scatter large around the regression line. In case of low fibre angle values, other criteria, such as knots or local fibre deviations limit the mechanical properties. Local aberrations of fibres aren't detected using ultrasound, as the detection is based on the RT-Profile. In case of local fibre deviation, other methods, such as thermal conductivity measurement, might be more attractive.

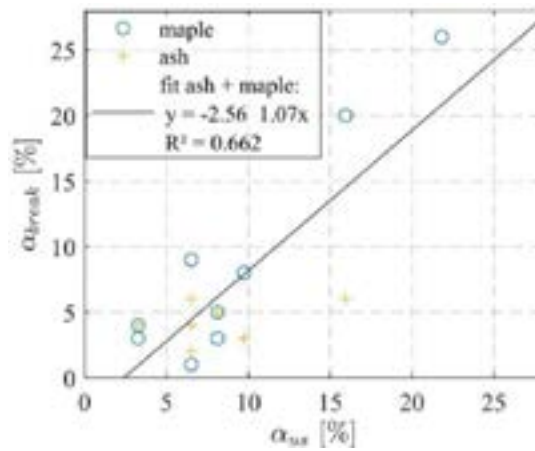


Figure 8: Relationship between grain angle determined from the ultrasound image and the grain angle after the failure

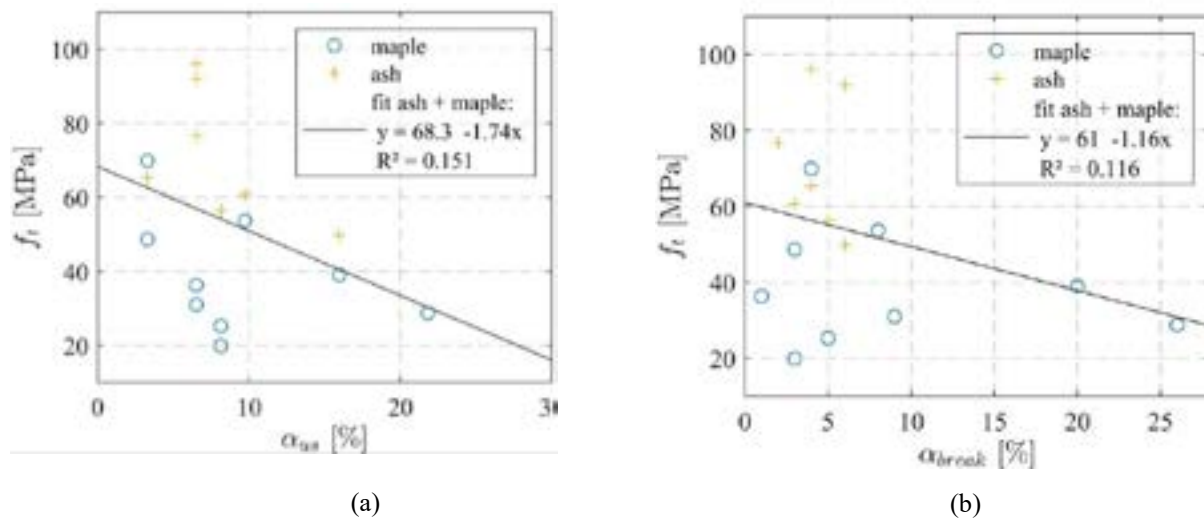


Figure 9: Relationship between (a) grain angle measured using ultrasound device and tensile strength and (b) manually measured grain angle after failure and tensile strength for European ash and maple

#### 4.3 MODULUS OF ELASTICITY PERPENDICULAR TO THE GRAIN

The relationship between ultrasound MOE perpendicular to the grain and tensile MOE longitudinal to the grain has been observed on the small (ash and maple) and on the large dataset (maple only). For small sample, no relationship between  $MOE_{dyn}$  perpendicular to the grain and mechanical properties (strength, stiffness) could be found. For the larger data set, measured with coarse grid, the ultrasound parameters - ultrasonic MOE perpendicular to the grain ( $E_{us,90}$ ) the velocity of ultrasound wave ( $v_{us}$ ) - show low to medium correlation to the tensile strength (Table 3). Maximum value shows the best correlation to tensile strength. Density improves the correlation of ultrasound velocity only slightly. Between  $E_{us,90,max}$  and  $E_0$  (Figure 10) no correlation can be found. The negative correlation and especially higher correlation of max. value of ultrasound velocity/ ultrasound MOE perp. to the grain can be explained as the values rather represent the local defects. The max. value of ultrasound velocity coincides with the presence of the knots (if any are present in a board), as the velocity in sound knots is greater compared to the clear wood.

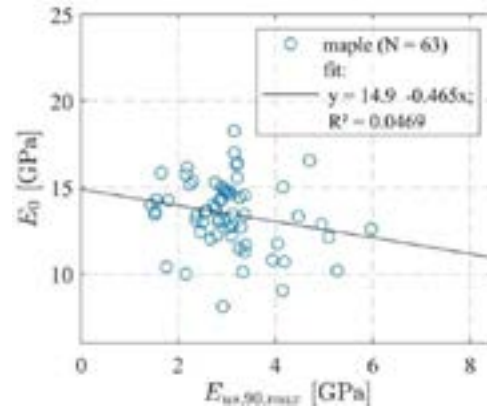


Figure 10: Relationship between the ultrasound MOE perpendicular to the grain and  $E_0$  for maple (*Acer spp.*) specimens ( $N = 63$ )

Table 3: Correlations between parameters of ultrasound wave and mechanical properties for maple (*Acer spp.*) ( $N = 63$ )

|                  | $E_{us,90,mean}$ | $E_{us,90,min}$ | $E_{us,90,max}$ | $v_{us,mean}$ | $v_{us,max}$ | $\rho$  | $E_0$  | $f_i$    |
|------------------|------------------|-----------------|-----------------|---------------|--------------|---------|--------|----------|
| $E_{us,90,mean}$ | 1                | 0.780**         | 0.778**         | 0.977**       | 0.777**      | 0.451** | -0.087 | -0.344** |
| $E_{us,90,min}$  |                  | 1               | 0.510**         | 0.763**       | 0.500**      | 0.510** | -0.004 | -0.207   |
| $E_{us,90,max}$  |                  |                 | 1               | 0.735**       | 0.986**      | 0.350** | -0.217 | -0.417** |
| $v_{us,mean}$    |                  |                 |                 | 1             | 0.764**      | 0.289** | -0.038 | -0.282*  |
| $v_{us,max}$     |                  |                 |                 |               | 1            | 0.255** | -0.189 | -0.391** |
| $\rho$           |                  |                 |                 |               |              | 1       | -0.101 | -0.268*  |
| $E_0$            |                  |                 |                 |               |              |         | 1      | 0.705**  |
| $f_i$            |                  |                 |                 |               |              |         |        | 1        |

Note: \* $p < 0.05$ , \*\* $p < 0.01$

#### 5. SUMMARY

Current study examined the opportunities of the ultrasound for defect detection in hardwood species ash and maple. Ultrasound is able to detect the strength-reducing characteristics, fibre orientation, the knot position and its size. Especially knottiness parameter shows high compliance with the manually measured knottiness. Also high correlation between knottiness and strength values could be achieved. Fibre deviation is an important parameter especially for the knot-free hardwood specimens. For a sample with knot and knot-free specimens tested in current study, no correlation between global fibre orientation (visually determined and using ultrasound) and strength could be found as in Frühwald and Schickhofer (2005). MOE perpendicular to the grain shows no relationship to the tensile MOE properties parallel to the grain. Due to the small sample size here, further tests on a large number of specimens are required. Further investigations are necessary, not only regarding the different wood species but also regarding the technical aspects of meeting industrial requirements.

#### ACKNOWLEDGEMENTS

This research was supported by the German Federal Ministry of Food and Agriculture (BMEL), grant no.: 22011913.

**REFERENCES**

- Bacher M (2008) Comparison of different machine strength grading principles. In: Proc. of Conference COST E53
- Bucur V (2006) *Acoustics of Wood*, 2<sup>nd</sup> Edition. Springer Series in Wood Science. Springer-Verlag Berlin Heidelberg, Berlin, Heidelberg
- Daval V, Pot G, Belkacemi M, Meriaudeau F, Collet R (2015) Automatic measurement of wood fiber orientation and knot detection using an optical system based on heating conduction. *Opt Express* 23(26):33529–33539. doi: 10.1364/OE.23.033529
- Ehrhart T, Steiger R, Frangi A (2018) A non-contact method for the determination of fibre direction of European beech wood (*Fagus sylvatica* L.). *Eur. J. Wood Prod.* 76(3):925–935. doi: 10.1007/s00107-017-1279-3
- EN 408 (2010) *Timber structures - Structural timber and glued laminated timber - Determination of some physical and mechanical properties*. CEN European Committee for Standardization, Brussels
- Frühwald K, Schickhofer G (2005) Strength grading of hardwoods. 14<sup>th</sup> International Symposium on Nondestructive testing of wood:198–210
- Giudiceandrea F (2005) Stress grading lumber by a combination of vibration stress waves and Xray scanning. In: 11<sup>th</sup> International Conference on Scanning Technology and Process Optimization in the Wood Industry (ScanTech 2005), pp 99–108
- Kabir MF, Schmoldt DL, Araman PA, Schafer ME, Lee S-M (2003) Classifying defects in pallet stringers by ultrasonic scanning. *Wood and Fiber Science* 35(3):341–350
- Kabir MF, Schmoldt DL, Schafer ME (2002) Time domain ultrasonic signal characterization for defects in thin unsurfaced hardwood lumber. *Wood and Fiber Science* 34
- Kovryga A, Schlotzhauer P, Stapel P, Militz H, van de Kuilen J-WG (2019) Visual and machine strength grading of European ash and maple for glulam application. *Holzforschung* 0(0):329. doi: 10.1515/hf-2018-0142
- Machado J, Sardinha R, Cruz H (2004) Feasibility of automatic detection of knots in maritime pine timber by acousto-ultrasonic scanning. *Wood Sci Technol* 38(4). doi: 10.1007/s00226-004-0224-x
- Nocetti M, Brunetti M, Bacher M (2016) Efficiency of the machine grading of chestnut structural timber: prediction of strength classes by dry and wet measurements. *Mater Struct* 49(11):4439–4450. doi: 10.1617/s11527-016-0799-3
- Olsson A, Oscarsson J, Serrano E, Källsner B, Johansson M, Enquist B (2013) Prediction of timber bending strength and in-member cross-sectional stiffness variation on the basis of local wood fibre orientation. *Eur. J. Wood Prod.* 71(3):319–333. doi: 10.1007/s00107-013-0684-5
- Olsson A, Pot G, Viguier J, Faydi Y, Oscarsson J (2018) Performance of strength grading methods based on fibre orientation and axial resonance frequency applied to Norway spruce (*Picea abies* L.), Douglas fir (*Pseudotsuga menziesii* (Mirb.) Franco) and European oak (*Quercus petraea* (Matt.) Liebl./*Quercus robur* L.). *Annals of Forest Science* 75(4):33529. doi: 10.1007/s13595-018-0781-z
- Ravenshorst GJP (2015) *Species independent strength grading of structural timber*. PhD. Technische Universiteit Delft, Delft.
- Sandoz JL (1989) Grading of construction timber by ultrasound. *Wood Sci Technol* 23(1):95–108. doi: 10.1007/BF00350611
- Schlotzhauer P, Wilhelm F, Lux C, Bollmus S (2018) Comparison of three systems for automatic grain angle determination on European hardwood for construction use. *Eur. J. Wood Prod.* 40:118. doi: 10.1007/s00107-018-1286-z
- Yaitskova N, Nadkernychmyy Y, Franjga R, Monroy R (2015) TUS: a breadboard for development of new wood grading algorithms using ultrasound
- Yaitskova N, van de Kuilen JW (2014) Time-of-flight modeling of transversal ultrasonic scan of wood. *J Acoust Soc Am* 135(6):3409–3415. doi: 10.1121/1.4873519